# Trace of the Interesting "V"-Shaped Dynamic Mechanism of Interactions between Water and Ionic Liquids

**Bingjie Sun,[†] Qiu Jin,[†] Lisha Tan,[†] Peiyi Wu,*[,†] and Feng Yan[‡]**

*The Key Laboratory of Molecular Engineering of Polymers (Ministry of Education) and Department of Macromolecular Science and Advanced Materials Laboratory, Fudan University, Shanghai 200433, PR China, and Key Laboratory of Organic Synthesis of Jiangsu Province, School of Chemistry and Chemical Engineering, Suzhou University, Suzhou 215123, PR China*

*Received: July 31, 2008*

The mixture of ionic liquid (1-butyl-3-methylimidazolium tetrafluoroborate, bmim$BF_4$) and water (2.5%, molar fraction) under isothermal conditions at 80 °C was investigated by FTIR spectroscopy and two-dimensional correlation infrared spectroscopy (2D-IR) methods. Three regions were focused: the OH stretching band of water (3755−3300 $cm^{-1}$), the stretching band of CH on the imidazole ring (3300−3020 $cm^{-1}$), and the BF stretching band of anions (1310−1260 $cm^{-1}$). During this process, water was gradually evaporated as time passed, which produced influences on the interactions among cations, anions, and water molecules. In the FTIR analysis, we found an interesting "V"-shaped changing trend in peak areas of the C−H on the imidazole ring and the B−F stretching band; the inflection of the system was 913 s, gained through the "moving window" method. A two-step variation was accordingly found during this process. Hydrogen bonds formed by water molecules with cations or water molecules with anions were destroyed by the reduction of water, making a fall in the former period of "V" process, while electrostatic interactions newly formed between anions and cations leading to a rise during the latter period of this course. In this paper, various conformations formed among cations, anions, and water molecules were clearly assigned, and we managed to trace the whole dynamic mechanism of this isothermal process by 2D-IR techniques.

## 1. Introduction

Ionic liquids are organic salts which are composed of asymmetric cations and anions and exist in molten state at low temperatures (<100 °C).[1−3] Numerous pairs of cations and anions can be selected to produce ionic liquids with various properties; therefore, they are also considered to be designer compounds.[4−9] Ionic liquids have lots of advantages, including negligible vapor pressures, high thermal stabilities, and excellent ionic conductivities.[4,10−12] Because of these merits and the "green" (environmentally friendly) potential, increasing interests are paid to the exploring researching of ionic liquids.[4,12−15] Ionic liquids are also quite useful as new fluids for lots of industrial products, like lithium ion batteries,[10,16,17] capacitors,[18−20] and fuel cell electrolytes.[21]

Figure 1 shows the general chemical structure of ionic liquids. It is widely known that the positive charge of cations mainly distributes on the imidazole ring while the alkyl chains are usually neutral.[22] So cations could be divided into two parts: the positively charged head and the alkyl tails. $C_nH_{2n+1}$ is often used to represent the alkyl chain of cations, where *n* refers to the number of carbon atoms on the alkyl chains. For example, $C_4H_9$ refers to $bmim^+$. There are three hydrogen atoms on the imidazole ring, which are usually numbered as $C_2$−H, $C_4$−H, and $C_5$−H.

Competitive van der Waals forces and electrostatic interactions exist among tails, heads, and anions. Short-range van der Waals force makes nonpolar tails aggregate and construct spatial heterogeneous domains, while long-range electrostatic interactions result in the charged homogeneous 3D network formed by heads interacting with anions.[23,24] Voth et al. found a micelle-like structure existing in dry ionic liquids by the molecular dynamics simulation method.[24,25] The micelle-like (network) structure could be influenced by the addition of water. Voth et al. observed this structure maintained when water content was 75−80% (molar fraction) but collapsed when water content is up to 91−95%.[24,26] This effect is due to hydrogen bonds between water and ions.[27,28]

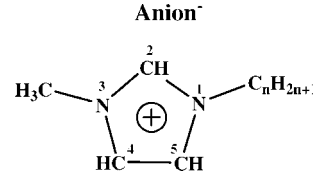


**Figure 1.** General chemical structure and atom numbering of ionic liquids. *n* refers to the number of carbon atoms on the alkyl chains.

Besides, further research told that both cations and anions of ionic liquids played a part in hydrogen bonds formation with water while the anions always dominated.[27−29] However, when the anion was hydrophobic, such as $PF_6^-$, interactions mainly occurred between water and the cations.[29] So far, a number of studies have been done on interactions between water and ionic liquids through experiments and simulations. Lendl-B discovered through IR and 2D-IR that water could interact with $BF_4^-$ contained ionic liquids in three forms of hydrogen bonds:[30] 1:1 ($BF_4^-$···water), 1:2 ($BF_4^-$···water···$BF_4^-$), and a cyclic water dimer interacting with $BF_4^-$. Using simulation methods, many researchers found that water could interact with $C_2$−H, $C_4$−H, and $C_5$−H of cation through hydrogen bonds, among which the

* Corresponding author: Fax +86-21-65640293; e-mail peiyiwu@fudan.edu.cn.
† Fudan University.
‡ Suzhou University.

10.1021/jp806805r CCC: $40.75 
Published on Web 10/18/2008

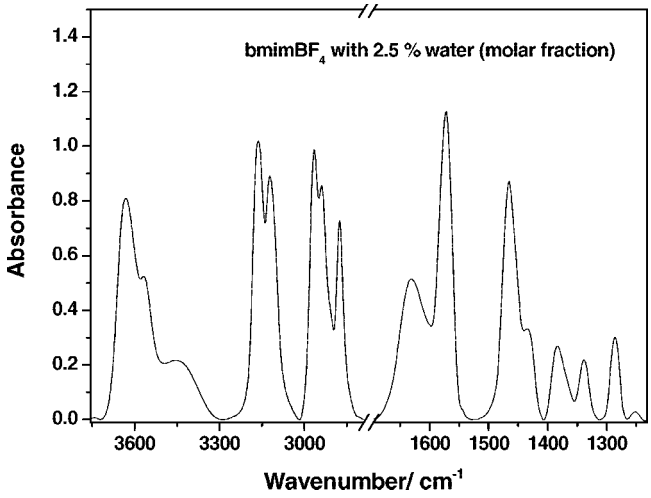


**Figure 2.** FTIR spectrum of bmimBF$_4$ with 2.5% water (molar fraction) at 80 °C.

interaction of water with C$_2$−H is the strongest,[29,31] as two neighboring N atoms have a relatively stronger electron-withdrawing ability to form the acidic C2−H bond.[29] People usually deal with C$_4$−H and C$_5$−H as a whole, probably because the properties of them are almost the same.[27,32]

Within various methods used to study these interactions inside ionic liquids, FTIR spectroscopy was proved to be quite powerful, owing to its high sensitivity to different molecular circumstances.[28,33−35] However, FTIR spectroscopy was not so effective when it comes to microstate's transform mechanism of ionic liquids, while the two-dimensional (2D) correlation spectroscopy technique is a perfect makeup.

Generalized two-dimensional (2D) correlation spectroscopy was originally proposed by Noda in 1993;[28] this spectroscopic method enables the investigation of the spectral intensity fluctuation under a disturbing variable which can be temperature,[36,37] time,[38] pH,[39,40] or concentration,[41] etc. The whole dynamic mechanism and specific event sequence of the system in perturbing process can thus be detailedly understood. 2D spectra are also able to improve the spectral resolution by capturing subtle information which is not obvious or overlapped in 1D FTIR spectra. To further improve 2D spectroscopy method, the moving window technique was proposed by Thomas in 2000.[42] By the moving window spectra, the critical transition point with the perturbation can be captured accurately. Ozaki et al. used such spectra to investigate the temperature dependence of glass-to-rubber transition phenomenon of the polymer.[43] Richardson used this technique to study the interfacial melting of thin ice.[44]

Though FTIR spectroscopy has been widely used to study interactions between ionic liquids and water molecules, most of these researches are interested in the interactions between water and anions, while the interactions of water or anions with different hydrogen atoms in cations have been limited studied; the region of anions were seldom studied; transition relationships or change orders among diverse interactions are not yet completely understood; in addition, most researches were focused on the addition process of water into ionic liquids, while the evaporation effect was less noted. In the present work, FTIR spectra were also employed, but it was proposed to roundly investigate the whole dynamic mechanism of interactions among the cations, anions, and water molecules during water evaporation at 80 °C with the help of 2D-IR and the moving window technique. Moreover, particular peak positions and integrated assignments of the cations, anions, and water with different interacted states were minutely studied as well.

## 2. Experimental Section

**2.1. Materials.** The ionic liquid 1-butyl-3-methylimidazolium tetrafluoroborate (bmimBF$_4$) was kindly supplied by Prof. Yan at Su Zhou University and used as received (see the chemical structures in Figure 1). Deionized water was added into ionic liquid with a concentration of 2.5% (molar ratio), and the solution was stirred for 1 week before FTIR experiments in order to ensure the complete blending of the mixture.

**2.2. Fourier Transform Infrared Spectroscopy.** The FTIR spectra were recorded with a 4 cm$^{-1}$ spectral resolution on a Nicolet Nexus 470 spectrometer equipped with a DTGS detector by signal-averaging 64 scans. Microscope $CaF_2$ windows, which have no absorption bands in the mid-IR region, were used to prepare a transmission cell.

The sample of bmimBF$_4$ with 2.5% deionized water (molar fraction) was maintained in an isothermal treatment process at 80 °C; variable spectra of sample during the this process were collected every 83 s from the very beginning to 9296 s. The baseline correct processing was performed by the OMNIC 7.3 software.

**2.3. Two-Dimensional Correlation Analysis.** Spectra recorded at an interval 83 s in isothermal experiments were selected in certain wavenumber ranges, and the generalized 2D correlation analysis was applied by the 2D Shige software composed by Shigeaki Morita (Kwansei-Gakuin University, Japan). The 2D correlation spectrum is shown in the center of the map, while the averaged 1D reference spectrum is at the left side and the top. In the 2D correlation maps, the red regions are defined as the positive correlation intensities, whereas the blue ones are regarded as the negative correlation intensities. The slice spectra of 2D maps were also plotted by the 2D Shige software. In moving window calculations of 2D maps, the window size of $2m + 1$ is refined to 25.

## 3. Results and Discussion

**3.1. FTIR Analysis.** Figure 2 shows the typical FTIR spectrum of the mixture of bmimBF4 and 2.5% water (molar fraction) at 80 °C. Three absorption bands were mainly studied: the O−H stretching band of water (3755−3300 cm$^{-1}$), the C−H stretching band of the imidazole ring (3300−3020 cm$^{-1}$), and the B−F stretching band of anions (1310−1260 cm$^{-1}$).[27,30] By analyzing these three bands, information on various interactions among water, cations, and anions could be learned.

FTIR spectra were continuously collected in the isothermal process of bmimBF$_4$ with 2.5% water (molar fraction) at 80 °C. In Figure 3a, the spectra of O−H stretching region are shown. Three obvious bands centered around 3642, 3566, and 3450 cm$^{-1}$ could be observed, all of which decrease with time. Considering the analyzing difficulties caused by the overlap of the three bands, we studied peak areas of them integratedly. Quantitative analysis of the changes in the peak area is shown in Figure 3b. The reduction of these peak areas are mainly owing to the evaporation of water.

Peaks in the range of 3300−3020 cm$^{-1}$ originated from C−H stretching vibrations of the imidazole ring are shown in Figure 4a. Peak areas of two partly overlapped bands around 3160 and 3120 cm$^{-1}$ are quantitatively analyzed in Figure 4b, in which an interesting "V"-shaped changing trend is found, probably resulting from changes of the ring C−H involved hydrogen bonds. Water gradually evaporated at 80 °C as time passed; therefore, hydrogen bonds formed between the ring C−H and

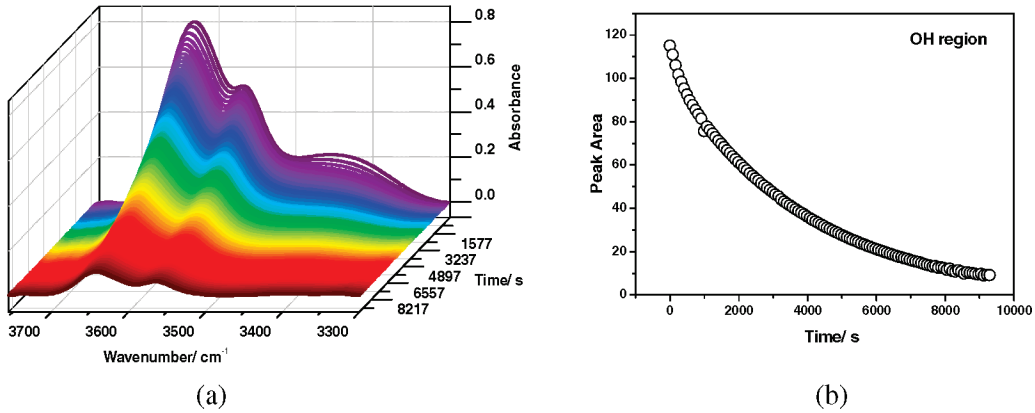


**Figure 3.** FTIR spectra (a) and peak areas (b) of bmimBF$_4$ with 2.5% water (molar fraction) in the $\nu$(O−H) region of 3755−3300 cm$^{-1}$ during isothermal process at 80 °C.

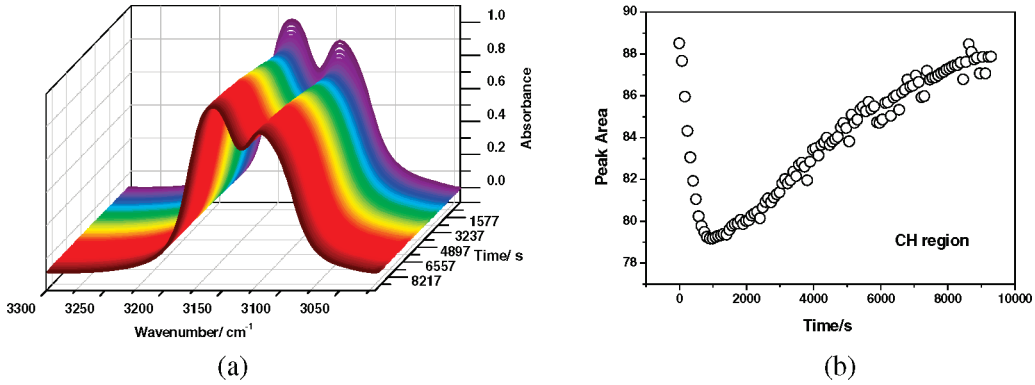


**Figure 4.** FTIR spectra (a) and peak areas (b) of bmimBF$_4$ with 2.5% water (molar fraction) in the $\nu$(C−H) region of 3300−3020 cm$^{-1}$ during isothermal process at 80 °C.

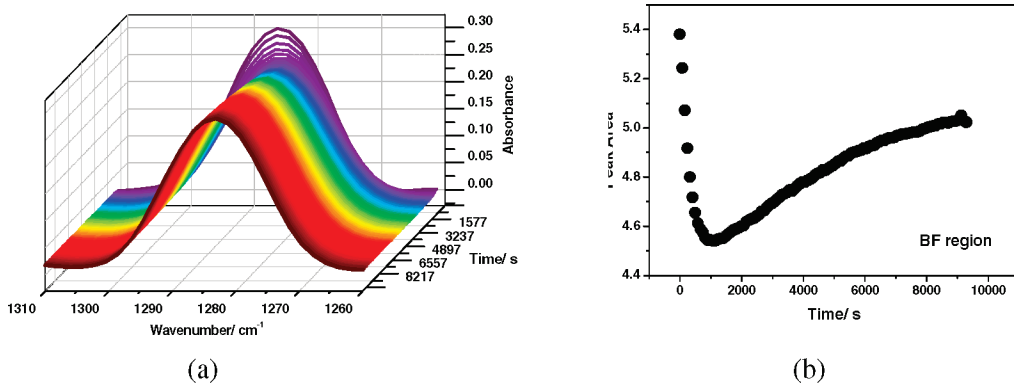


**Figure 5.** FTIR spectra (a) and peak areas (b) of bmimBF$_4$ with 2.5% water (molar fraction) in the $\nu$(B−F) region of 1310−1260 cm$^{-1}$ during isothermal process at 80 °C.

water were destroyed accordingly, which made the ring C−H free and sequentially cause a fall in the peak area. A similar situation might happen to the anions as well. When the number of "free" cations and anions reached a certain content, they would interact with each other because of the strong electrostatic forces, leading to the latter rise in Figure 4b.

The BF stretching band centered at 1280 cm$^{-1}$ is shown in Figure 5a. According to our previous expectation, a "V" shape could also be found in the change of the peak areas of this anion related region in Figure 5b. A further explanation of these interesting phenomena will be discussed in the following 2D analysis.

**3.2. Two-Dimensional Correlation Analysis.** The red and blue areas in the 2D-IR correlation contour maps represent positive and negative cross-peaks, respectively. The 2D-IR correlation spectra are characterized by two independent wavenumber axes ($\nu_1$, $\nu_2$) and a correlation intensity axis. Generally, two types of spectra, 2D synchronous and 2D asynchronous, could be gained. The correlation intensity in the synchronous and asynchronous maps reflects the relative degree of in-phase and out-of phase response, respectively.

The 2D synchronous spectra are symmetric with respect to the diagonal line in the correlation map. Peaks appearing along the diagonal are called "autopeaks", and their symbols are always positive; autopeaks are thought to represent the degree of autocorrelation of perturbation-induced molecular vibrations and always change greatly under environmental perturbations. Off-diagonal peaks are cross-peaks ($\Phi(\nu_1,\nu_2)$), which may be positive or negative, represent the coincidental changes of spectra intensity variations measured at $\nu_1$ and $\nu_2$. Positive cross-peaks (the symbol of $\Phi(\nu_1,\nu_2)$ is positive) demonstrates intensity variations of the two peaks at $\nu_1$ and $\nu_2$ take place in the same

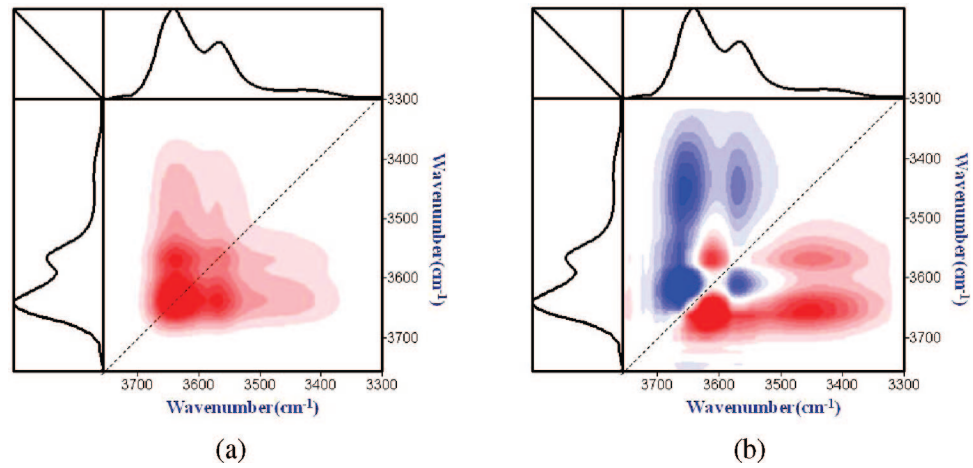


**Figure 6.** Synchronous (a) and asynchronous (b) maps of $bmimBF_4$ with 2.5% water (molar fraction) in the $\nu$(O−H) region of 3755−3300 $cm^{-1}$ during isothermal process at 80 °C.

**TABLE 1: Change Sequences within $\nu$(O−H) Region, Calculated from 2D Maps and Slice Spectra of $bmimBF_4$ with 2.5% Water (Molar Fraction) during Isothermal Process at 80 °C[a]**

| ($\nu_1$, $\nu_2$)/$cm^{-1}$ | synchronous | asynchronous | sequence/ $cm^{-1}$ |
|---|---|---|---|
| (3656, 3610) | + | − | 3610 → 3656 |
| (3656, 3450) | + | − | 3450 → 3656 |
| (3565, 3450) | + | − | 3450 → 3565 |
| (3610, 3565) | + | + | 3610 → 3565 |
| (3610, 3450) | + | − | 3450 → 3610 |
| (3743, 3643) | + | + | 3743 → 3643 |

[a] 3743 → 3643 $cm^{-1}$; 3450 → 3610 → 3656, 3565 $cm^{-1}$; $\nu$(OH) in hydrogen bond of water with $C_{45}$−H → $\nu$(OH) in hydrogen bond of water with $C_2$−H; $\nu$(OH) in water−water interaction within cyclic water dimer interacting with $BF_4^-$ → $\nu$(OH) in water−$BF_4^-$ hydrogen bond in cyclic water dimer interacting with $BF_4^-$ → $\nu$(OH) in hydrogen bond of $BF_4^-\cdots HOH\cdots BF_4$.

direction (both increase or decrease) under a certain environmental perturbation, while the negative cross-peaks (the symbol of $\Phi(\nu_1,\nu_2)$ is negative) help to infer intensities of the two peaks at $\nu_1$ and $\nu_2$ change in opposite directions (one increase while the other one decrease) with perturbation.

The 2D asynchronous spectra are asymmetric with respect to the diagonal line in the correlation map. Unlike the synchronous spectra, there is no autopeak in asynchronous spectra, and only off-diagonal cross-peaks would appear, which can be either positive or negative. Intensity of the asynchronous spectrum cross-peak ($\Psi(\nu_1,\nu_2)$) represents sequential or successive changes of spectral intensities observed at $\nu_1$ and $\nu_2$. With the cross-peaks both in synchronous and asynchronous maps, we can get the specific order of the spectral intensity changes taking place while the sample is subjected to an environmental perturbation. According to Noda's rule,[45−47] when $\Phi(\nu_1,\nu_2) > 0$, if $\Psi(\nu_1,\nu_2)$ is positive (red area), band $\nu_1$ will vary prior to band $\nu_2$; if $\Psi(\nu_1,\nu_2)$ is negative (blue area), band $\nu_1$ will vary after $\nu_2$. However, this rule is reversed when $\Phi(\nu_1,\nu_2) < 0$. Briefly, if the symbols of the cross-peak in the synchronous and asynchronous maps are the same (both positive or both negative), band $\nu_1$ will vary prior to band $\nu_2$, while if the symbols of the cross-peak are different in the synchronous and asynchronous spectra (one positive and the other one is negative), band $\nu_1$ will vary after $\nu_2$ under the environmental perturbation. Sometimes, cross-peaks are not so significant that they cannot be observed clearly in either synchronous or asynchronous map, while the slice spectra also drawn by Shige software will be quite helpful in solving such problems.

***3.2.1. The $\nu$(O−H) Region of 3755−3300 $cm^{-1}$.*** 2D synchronous and asynchronous spectra in the $\nu$(O−H) region of $bmimBF_4$ with 2.5% water (molar fraction) under the isothermal condition at 80 °C are depicted in Figure 6. In the synchronous spectrum, two autopeaks are found at 3643 and 3565 $cm^{-1}$. As described above, the autopeak manifests that the corresponding peak changes greatly with molecular environmental variations. So, the synchronous data imply that bands at 3643 and 3565 $cm^{-1}$ are both susceptible to water reduction in the relatively high temperature.

In the corresponding asynchronous spectrum of Figure 6b, we could easily find five cross-peaks: (3656, 3610), (3656, 3450), (3565, 3450), (3610, 3565), and a little one at (3743, 3643) $cm^{-1}$. As a result, we could deduce that there may be six different water O−H involved conformations in this $bmimBF_4$ with 2.5% water (molar fraction) system, represented by peaks appearing at 3743, 3656, 3643, 3610, 3565, and 3450 $cm^{-1}$, respectively. In Lendl-B's previous work,[30] the conformation of a cyclic water dimer interacting with $BF_4^-$ was found, and there are two kinds of hydrogen bonds in it: one is formed between two water molecules, and the other one is formed between water and $BF_4^-$; 3450 and 3610 $cm^{-1}$ were assigned to the O−H stretching vibration of these two hydrogen bonds, respectively. Additionally, bands of 3656 and 3565 $cm^{-1}$ have been assigned to the asymmetric and symmetric vibrations of the O−H in hydrogen bonds of $BF_4^-\cdots water\cdots BF_4^-$. Peaks at 3743 and 3643 $cm^{-1}$ found in the present work have never been reported before, as their higher wavenumbers reflect weaker hydrogen bonds; the band at 3743 $cm^{-1}$ could be assigned to the O−H stretching vibrations in hydrogen bonds formed between water and $C_{4,5}$−H, while 3643 $cm^{-1}$ to water with $C_2$−H.

To reveal the transform sequence of these conformations, we calculate the cross-peaks among them in 2D maps and slice spectra, results of which are shown in Table 1. The transform order of these peaks was finally discerned as 3743 → 3643 $cm^{-1}$; 3450 → 3610 → 3656, 3565 $cm^{-1}$ (the arrow "→" means "changes prior to"). In light of these change sequences and peak assignments gained above, we finally conclude that in the mixture of $bmimBF_4$ and water (2.5%, molar fraction), hydrogen bonds of $C_{4,5}$−H and water are much weaker than that of $C_2$−H and water; therefore, the former interactions begin to collapse earlier than the latter. Moreover, two kinds of hydrogen bonds

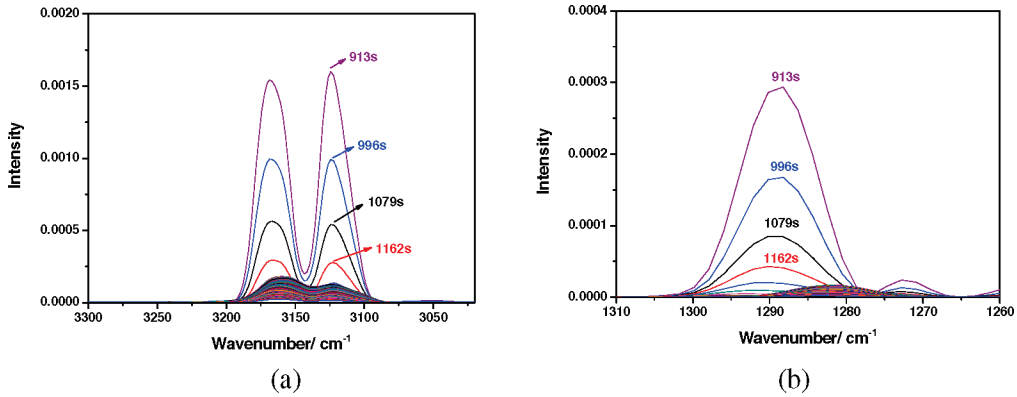


**Figure 7.** Moving window spectra of $\nu$(CH) (a) and $\nu$(BF) (b) regions of bmim$BF_4$ with 2.5% water (molar fraction) during isothermal process at 80 °C.

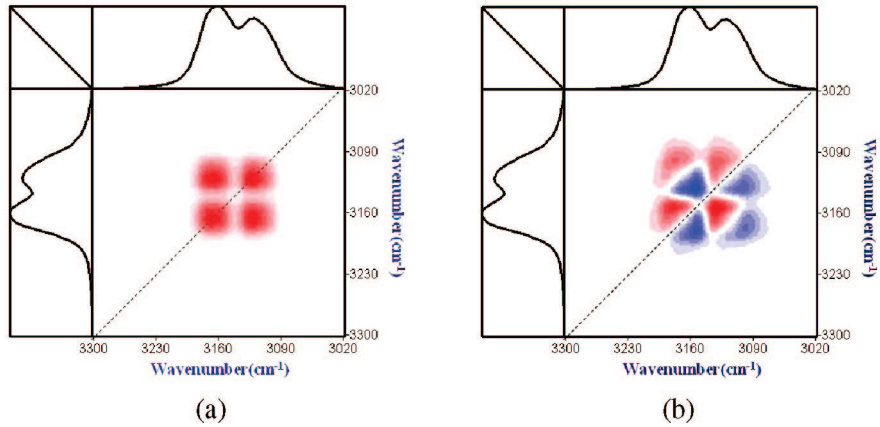


**Figure 8.** Synchronous (a) and asynchronous (b) maps of bmim$BF_4$ with 2.5% water (molar fraction) in $\nu$(C−H) region of 3300−3020 $cm^{-1}$ during isothermal period of 0−913 s at 80 °C.

**TABLE 2: Change Sequences within $\nu$(C−H) Region, Calculated from 2D and Slice Spectra of bmim$BF_4$ with 2.5% Water (Molar Fraction) during Isothermal Period of 0−913 s at 80 °C[a]**

| ($\nu_1$, $\nu_2$)/$cm^{-1}$ | synchronous | asynchronous | sequence/ $cm^{-1}$ |
|---|---|---|---|
| (3174, 3126) | + | + | 3174 → 3126 |
| (3149, 3126) | + | − | 3126 → 3149 |
| (3149, 3097) | + | + | 3149 → 3097 |

[a] 3174 → 3126 → 3149 → 3097 $cm^{-1}$; $\nu$(C−H) in hydrogen bond of $C_{4,5}$−H with water → $\nu$(C−H) in hydrogen bond of $C_2$−H with water → $\nu$(C−H) in $C_{4,5}$−H interacting with $F^-$ → $\nu$(C−H) in $C_2$−H interacting with $F^-$.

in $BF_4^-$ involved cyclic water dimer change differently, in which water−water interactions break prior to water−anion hydrogen bonds; the symmetric structure of $BF_4^-$···HOH··· $BF_4^-$ is so stable that the hydrogen bond existing in this structure would collapse only with vast water reduction.

***3.2.2. The ν(C−H) Region of 3300−3020 cm⁻¹.*** As seen in Figures 4b and 5b, peak areas of cations and anions were found to change with an interesting V shape during the isothermal process at 80 °C, from which we could tentatively infer that a two-step variation happened. In order to analyze the microdynamic mechanism of whole course more clearly, it is important to seize the inflection of this V shape change. The moving window method is quite helpful in distinguishing such a critical point. Figure 7a is the moving window spectrum calculated in the cation-related region (3300−3020 $cm^{-1}$), from which the critical change point at 913 s can be observed clearly, showing that two kinds of changes take place: the first step of the change starts at the very beginning of the isothermal process and ends at 913 s, while the second step happens during the following period. Figure 7b is the moving window spectrum of the anion-related region (1310−1260 $cm^{-1}$), which also shows a significant transition point at 913 s. Considering this simultaneous phenomenon of Figure 7a,b, we can infer that the two-step changes may be mainly caused by interactions between cations and anions. To further confirm this deduction, 2D maps of cations and anions related vibration bands are drawn in time domains of 0−913 s and 996 s−end, respectively.

*1. 0−913 s.* Figure 8 presents the synchronous (a) and asynchronous (b) maps of bmim$BF_4$ with 2.5% $H_2O$ (molar fraction) in the region of 3300−3020 $cm^{-1}$ for 0−913 s of the isothermal process at 80 °C, from which we can get an insight into changes happening to cations in the first step.

It is well-known that both $C_2$−H and $C_{4,5}$−H on the ring can interact with water through hydrogen bonds and with anions through electrostatic interactions.[23,24,27,28] Hence, there are at least four different conformations. However, their corresponding vibration peaks were seldom assigned in previous FTIR studies because of difficulties caused by the overlapping of peaks. 2D-IR maps are thus introduced to conquer this puzzle.

In the asynchronous map of Figure 8b, cross-peaks exist in four main bands centered at 3174, 3149, 3126, and 3097 $cm^{-1}$, indicating the existence of four kinds of C−H involved microstructures, which is consistent with our anticipation.

That the wavenumber of $\nu$(CH) related to $C_2$−H interacting with anions is lower than that of $C_{4,5}$−H and anions lies in the following two facts. First, the electrostatic interaction of $C_2$−H with anion is stronger than that of $C_{4,5}$−H with anion,[29,31] and

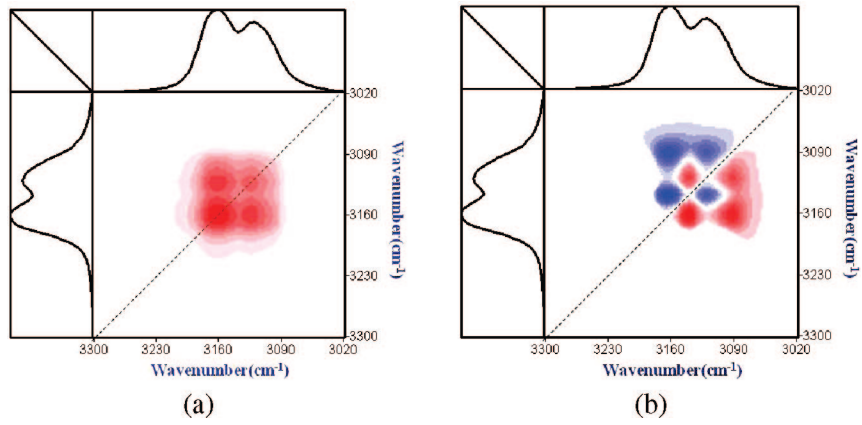


**Figure 9.** Synchronous (a) and asynchronous (b) maps of $bmimBF_4$ with 2.5% water (molar fraction) in $\nu$(C−H) region of 3300−3020 $cm^{-1}$ during isothermal period of 996 s−end at 80 °C.

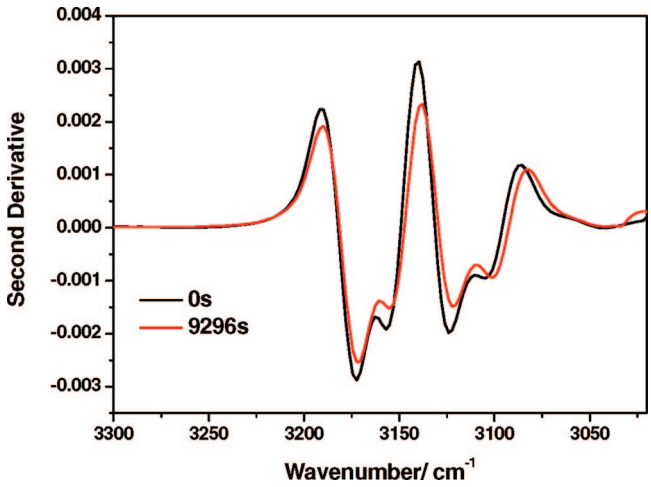


**Figure 10.** Second-derivative spectra of $bmimBF_4$ with 2.5% water in $\nu$(C−H) region of 3300−3020 $cm^{-1}$ before isothermal treatment (0 s) and after isothermal treatment of 9296 s.

**TABLE 3: Change Sequences within $\nu$(C−H) Region, Calculated from 2D and Slice Spectra of $bmimBF_4$ with 2.5% Water during Isothermal Period of 996 s−End at 80 °C[a]**

| ($\nu_1$, $\nu_2$)/$cm^{-1}$ | synchronous | asynchronous | sequence/ $cm^{-1}$ |
|---|---|---|---|
| (3139, 3091) | + | − | 3091 → 3139 |
| (3139, 3122) | + | + | 3139 → 3122 |
| (3164, 3122) | + | − | 3122 → 3164 |

[a] 3091→ 3139 → 3122 → 3164 $cm^{-1}$; $\nu$(C−H) in $C_2$−H interact with $F^-$ → $\nu$(C−H) in $C_{4,5}$−H interact with $F^-$ → $\nu$(C−H) in hydrogen bond of $C_2$−H with water → $\nu$(C−H) in hydrogen bond of $C_{4,5}$−H with water.

second, the C−H stretching vibrations of the imidazolium ring are closely related to the strength of interactions between cations and anions, that the stronger the electrostatic interactions are, the lower the wavenumber of $\nu$(CH) of the cation ring will be. The same situation is also suited for $\nu$(BF).[27]

Therefore, the peak centered at the lowest wavenumber of 3097 $cm^{-1}$ could be assigned to $\nu$(CH) of $C_2$−H interacting with $BF_4^-$, where the addition of water may lead this peak blue shift to a little higher position,[27] and 3126 $cm^{-1}$ could be assigned to $\nu$(CH) of $C_2$−H with water hydrogen bonds. Similarly, 3149 and 3174 $cm^{-1}$ could be assigned to $C_{4,5}$−H interacting with $BF_4^-$ and $C_{4,5}$−H with water hydrogen bonds, respectively.

To make their transformation relationships clear, cross-peaks at (3174, 3126), (3149, 3126), and (3149, 3097) $cm^{-1}$ were calculated in 2D maps and slice spectra (not shown in this paper). Results are shown in Table 2, from which we could obtain the whole transition sequence of these four different conformations as follows: hydrogen bond of $C_{4,5}$−H with water → hydrogen bond of $C_2$−H with water → $C_{4,5}$−H interacting with $BF_4^-$ → $C_2$−H interacting with $BF_4^-$. Namely, hydrogen bonds between cations and water will be broken as water evaporating at 80 °C, and then new interactions between cations and anions will be constructed. Since the hydrogen bond formed between $C_{4,5}$−H and water is much weaker than that between $C_2$−H and water, $C_{4,5}$−H will get rid of such a hydrogen bond and become free earlier; then free C−H atoms will prefer to interact with free anions set out as water reducing (discussed in later part). As free $C_{4,5}$−H appears earlier than $C_2$−H, it will interact with $BF_4^-$ prior to $C_2$−H.

*2. 996 s−End.* With the V shape curve described above, different microstate changes were believed to occur in the posterior isothermal process from 996 s to the end. Figure 9 is the synchronous and asynchronous maps of $bmimBF_4$ with 2.5% $H_2O$ (molar fraction) in the region of 3300−3020 $cm^{-1}$ during this corresponding period.

Same as the former period, four bands were found as well. But all of these peaks have little red shift, which is illuminated in the second-derivative spectra of Figure 10. The red shift is mainly caused by the evaporation of water and by the enhancement of interactions between cations and anions.[27] Through analyzing the cross-peaks, the change sequence of this period can be concluded as 3091 → 3139 → 3122 → 3164 $cm^{-1}$ (shown in Table 3). Compared with Table 2, we note that conformations related to cations change in different orders within these two periods.

In the former period, hydrogen bonds are broken before C−H atoms interacting with $BF_4^-$; during the latter period, however, C−H atoms interact with $BF_4^-$ earlier than hydrogen bonds of C−H with water collapse. Therefore, it could be concluded that 0−913 s is the main period of the water evaporation, little water will be left after that, while in the latter period of 996 s to the end, interactions between free cations and anions will be constructed. In addition, as the electrostatic interactions between $C_2$−H and $BF_4^-$ are much stronger than $C_{4,5}$−H and $BF_4^-$, free $C_2$−H atoms will prefer to interact with anions much quicker than $C_{4,5}$−H. Water molecules left in the system are still involved in hydrogen bonds, but so scanty that it no longer changes significantly, and the stronger tendency of $C_2$−H interacting with anions leads to collapse of hydrogen bonds

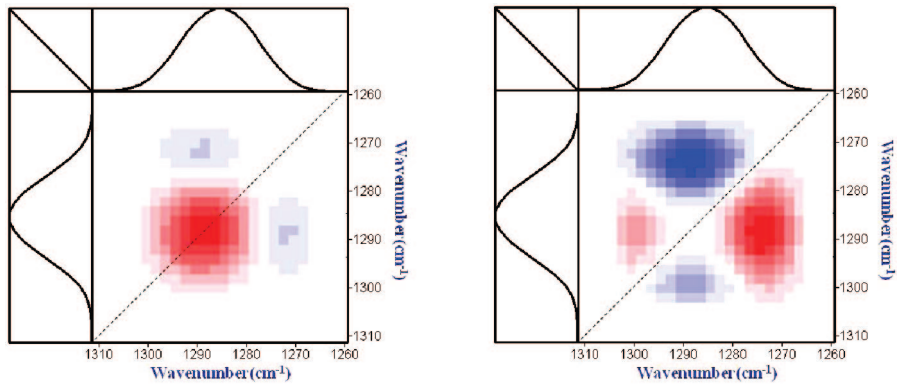


**Figure 11.** Synchronous (a) and asynchronous (b) maps of bmim$BF_4$ with 2.5% water (molar fraction) in $\nu$(B−F) region of 1310−1260 $cm^{-1}$ during isothermal period of 0−913 s at 80 °C.

**TABLE 4: Change Sequences within $\nu$(B−F) Region, Calculated from 2D and Slice Spectra of bmim$BF_4$ with 2.5% Water (Molar Fraction) during Isothermal Period of 0−913 s at 80 °C[a]**

| ($\nu_1$, $\nu_2$)/$cm^{-1}$ | synchronous | asynchronous | sequence/ $cm^{-1}$ |
|---|---|---|---|
| (1297, 1288) | + | + | 1297 → 1288 |
| (1288, 1274) | − | − | 1288 → 1274 |

[a] 1297 → 1288→ 1274 $cm^{-1}$; $\nu$(B−F) in hydrogen bond of $BF_4^-$ with water → $\nu$(B−F) in $BF_4^-$ interacting with $C_{4,5}$−H → $\nu$(B−F) in $BF_4^-$ interacting with $C_2$−H.

between $C_2$−H and water earlier than that of water with $C_{4,5}$−H. It is known that the intensities of $\nu$(CH) band are related to the strength of interactions between cations and anions, which will greatly fortify in the posterior period according to 2D analysis; hereby the increasing peak areas of $\nu$(CH) in Figure 4b are caused by enhanced interactions between cations and anions in this system.

***3.2.3. The ν(B−F) Region of 1310−1260 cm⁻¹.*** *1. 0−913 s.* Since the transition point of $\nu$(BF) band is the same with that of the C−H band, the 1310−1260 $cm^{-1}$ region was divided into 0−913 s and 996 s−end as well. Figure 11 shows the synchronous and asynchronous maps of bmim$BF_4$ with 2.5% $H_2O$ (molar fraction) in the region of 1310−1260 $cm^{-1}$ during 0−913 s of the isothermal process at 80 °C.

Anions can interact with water, $C_2$−H and $C_{4,5}$−H, so there were expected to be three peaks in this region. In the asynchronous map of Figure 11b, cross-peaks exist in three main bands centered at 1297, 1288, and 1274 $cm^{-1}$. Because the addition of water would make a blue shift of $\nu$(BF),[27] the peak at the highest wavenumber of 1297 $cm^{-1}$ can be assigned to the stretching vibration of B−F interacting with water; while for $BF_4^-$ interacting with cations, based on the relationship between interaction intensity and wavenumber magnitude mentioned in the analysis of the C−H band,[27] the stronger force between $BF_4^-$ and $C_2$−H should have a lower wavenumber vibration peak at 1274 $cm^{-1}$, while weaker forced $BF_4^-$ with $C_{4,5}$−H at higher wavenumber of 1288 $cm^{-1}$.

Cross-peaks are analyzed with 2D maps and slice spectra, and the results are shown in Table 4. The change sequence of these three conformations is gained as follows: 1297 → 1288 → 1274 $cm^{-1}$ (hydrogen bond of $BF_4^-$ with water → $BF_4^-$ interact with $C_{4,5}$−H → $BF_4^-$ interact with $C_2$−H). As the isothermal time increases, water gradually vapors, so hydrogen bonds formed between $BF_4^-$ and water are destroyed earliest. After that free anions will interact with free C−H of cations, by former concluded change sequence of C−H region within 0−913 s, we know that hydrogen bond between $C_{4,5}$−H and water breaks before that between $C_2$−H and water; therefore, free $C_{4,5}$−H appears in the system earlier and interacts with $BF_4^-$ prior to free $C_2$−H.

*2. 996 s−End.* There might be different change sequence after 996 s according to the V shape in Figure 5b. The synchronous and asynchronous maps of bmim$BF_4$ with 2.5% $H_2O$ (molar fraction) in the region of 1310−1260 $cm^{-1}$ are shown in Figure 12. Three bands are also found but with little red shift compared to the former period. Change sequence in this time domain is concluded in Table 5 as 1297 → 1274 → 1282 $cm^{-1}$. The breakage of hydrogen bonds related to $BF_4^-$ with water happens first as in former period of 0−913 s, but in the same change period of cations, the dehydration of C−H groups takes place later than the interaction of cations and anions forms; that is because the interaction between water and $BF_4^-$ is much stronger than that between water and cations, and hydrogen bond within $BF_4^-\cdots HOH\cdots BF_4^-$ is quite stable as well. As a result, free $BF_4^-$ has much more difficulties in running out of these hydrogen bonds with water than cation does.

In addition, compared with Table 4, different change sequences lie in $BF_4^-$ interacting with $C_2$−H varied prior to $C_{4,5}$−H in the latter period, which is consistent with results found in the C−H region.

Through the above 2D-IR analysis, we could clearly understand the molecular leveled interactions among cations, anions, and water molecules in the system. For a more intuitionistic understanding of them, we illustrated all the proved and assigned structures in Figure 13. Water could interact with cations and form hydrogen bonds through $C_2$−H, $C_4$−H, and $C_5$−H, which is represented by I, II, and III in Figure 13, respectively; water also interacts with anions in two types as i and ii: i is related to $BF_4^-\cdots HOH\cdots BF_4^-$ hydrogen-bonding structure, while ii is related to $BF_4^-$ interacting with the cyclic water dimer structure, where two kinds of hydrogen bonds (water with water and water with $BF_4^-$) exist. The strongest interactions in the system are electrostatic forces between anions and cations; $BF_4^-$ could interact with $C_2$−H, $C_4$−H, and $C_5$−H, which is represented by conformation 1, 2, and 3, respectively.

Through summarizing all change sequences gained in 2D-IR analysis, we could get a whole view of the microdynamic mechanism among all structures during the isothermal process at 80 °C on a molecular level. 0−913 s is the main period that most water is vaporized; herein the relatively weaker II and III

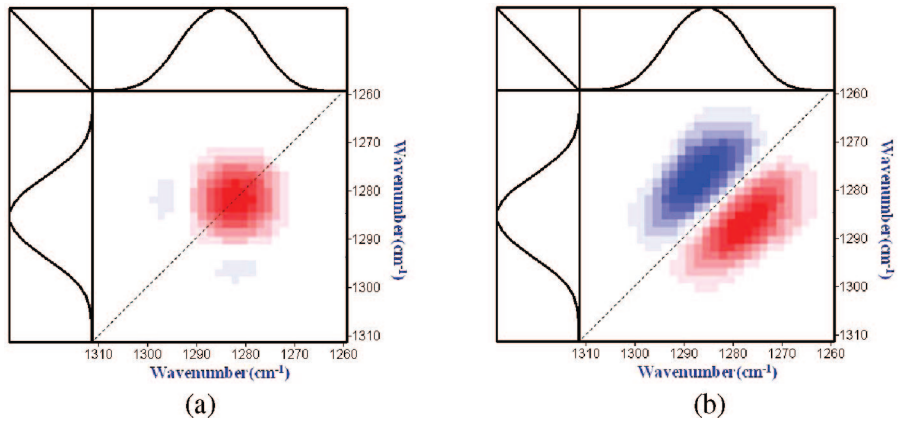


**Figure 12.** Synchronous (a) and asynchronous (b) maps of $bmimBF_4$ with 2.5% water (molar fraction) in $\nu$(B−F) region of 1310−1260 $cm^{-1}$ during isothermal period of 996 s−end at 80 °C.

**TABLE 5: Change Sequences within $\nu$(B−F) Region, Calculated from 2D and Slice Spectra of $bmimBF_4$ with 2.5% Water (Molar Fraction) during Isothermal Period of 996 s−End at 80 °C[a]**

| ($\nu_1$, $\nu_2$)/$cm^{-1}$ | synchronous | asynchronous | sequence/ $cm^{-1}$ |
|---|---|---|---|
| (1297, 1274) | − | − | 1297 → 1274 |
| (1282, 1274) | + | − | 1274 → 1282 |

[a] 1297 → 1274→ 1282 $cm^{-1}$; $\nu$(B−F) in hydrogen bond of $BF_4^-$ with water → $\nu$(B−F) in $BF_4^-$ interacting with $C_2$−H → $\nu$(B−F) in $BF_4^-$ interacting with $C_{4,5}$−H.

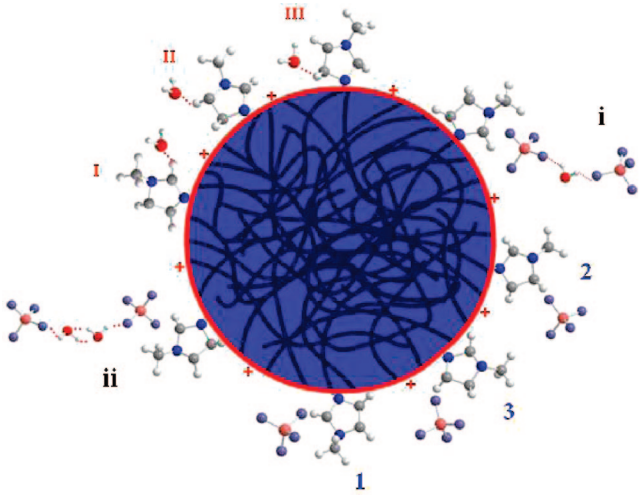


**Figure 13.** Various structures and interactions among cations ($bmim^+$), anions ($BF_4^-$), and water molecules existing in the mixture of $bmimBF_4$ with 2.5% water (molar fraction). The big blue ball area represents tail aggregated domains of alkyl chains of $bmim^+$; imidazole heads locate outside of tail blue ball can interact with water molecules through hydrogen bonds of I ($C_2$−H with water), II ($C_4$−H with water), and III ($C_5$−H with water); cations could also interact with anions by electrostatic forces as 1 ($C_2$−H with $BF_4^-$), 2 ($C_4$−H with $BF_4^-$), and 3 ($C_5$−H with $BF_4^-$). $BF_4^-$ anions interact with water molecules through hydrogen bonds of i ($BF_4^-\cdots HOH\cdots BF_4^-$) and ii (cyclic water dimer interacting with $BF_4^-$) in the current system.

structures are destroyed earlier than I; ii is not as stable as i, and water−water hydrogen bond in ii is broken prior to hydrogen bond of water−$BF_4^-$, after that i collapse. Only a few free cations and anions molecules are set out during this period, and the earlier appeared $C_{4,5}$−H interacts with $BF_4^-$ prior to $C_2$−H, namely conformations 2 and 3 appear earlier than 1 in this period.

During the following period of 996 s−end less water is left, much more cations and anions are free and interact with each other through electrostatic forces. Because of stronger interactions, $C_2$−H prefers to interact with anions than $C_{4,5}$−H does; namely, conformation 1 constructs much earlier than 2 and 3 in this period.

## 4. Conclusions

The 2D-IR and moving window methods both provide a vivid characterization of the evolution process of $bmimBF_4$ with continuous evaporation of water. Obvious changes take place in three regions: OH stretching vibration region (3755−3300 $cm^{-1}$), CH stretching vibration region (3300−3020 $cm^{-1}$), and BF stretching region (1310−1260 $cm^{-1}$).

In 3755−3300 $cm^{-1}$, peak area of OH stretching vibration decreases gradually as water evaporates. 2D-IR results suggest that hydrogen bond between water and $C_{4,5}$−H collapses earlier than the relatively stronger hydrogen bond connecting water and $C_2$−H; water−water hydrogen bond in $BF_4^-$ involved cyclic water dimer dissociates followed by the breakage of $BF_4^-$−water hydrogen bond also in this cyclic water dimer structure. At last, the left scanty water is inadequate to hold the stable hydrogen bond of $BF_4^-\cdots HOH\cdots BF_4^-$.

Differently, peak areas of 3300−3020 and 1310−1260 $cm^{-1}$ both take on an interesting V shape, indicating a two-step change of CH on the imidazole ring and BF stretching vibration as water evaporates continually. With the aid of the moving window technique, we find a critical point of 913 s, which divides our following study into two parts: 0−913 s and 996 s−end.

For the CH stretching vibration, during 0−913 s, as water is comparatively much, breakage of hydrogen bond between water and cations occurs first, and then comes the interaction of released cations with anions. However, during 996 s−end, scanty water remaining in the system makes loss of water indistinctively, which induces an opposite change sequence as in 0−913 s.

For the BF stretching vibration mode, during 0−913 s, relatively adequate water leads the hydrogen bond between $BF_4^-$ and water to break very easily. Then the set-out $BF_4^-$ interacts with $C_{4,5}$−H prior to $C_2$−H, for $C_{4,5}$−H becomes free earlier. The transform sequence of 996 s−end differs from that of 0−913 s in part. Although water left during 996 s−end is little, the hydrogen bond between water and $BF_4^-$ breaks first whatever. Afterward, $BF_4^-$ prefers to interact with $C_2$−H rather than $C_{4,5}$−H, similar to the CH region.

**Acknowledgment.** The authors gratefully acknowledge the financial support by the National Science of Foundation of China

(NSFC) (Nos. 20774022, 20573022, 20425415, 20490220), the "Leading Scientist" Project of Shanghai (No. 07XD14002), the National Basic Research Program of China (2005CB623800), and the PHD Program of MOE (20050246010).

## References and Notes

(1) Rebelo, L. P. N.; Lopes, J. N. C.; Esperanca, J. M. S. S.; Filipe, E. *J. Phys. Chem. B* **2005**, *109*, 6040.
(2) Sloutskin, E.; Lynden-Bell, R. M.; Balasubramanian, S.; Deutsch, M. *J. Chem. Phys.* **2006**, *125*, 174715.
(3) Yamaguchi, T.; Nagao, A.; Matsuoka, T.; Koda, S. *J. Chem. Phys.* **2003**, *119*, 11306.
(4) Welton, T. *Chem. Rev.* **1999**, *99*, 2071.
(5) Yan, F.; Texter, J. *Angew. Chem., Int. Ed.* **2007**, *46*, 2440.
(6) Yan, F.; Texter, J. *Chem. Commun.* **2006**, 2696.
(7) Seddon, K. R. *Nat. Mater.* **2003**, *2*, 363.
(8) Castner, E. W.; Wishart, J. F.; Shirota, H. *Acc. Chem. Res.* **2007**, *40*, 1217.
(9) Dupont, J.; de Souza, R. F.; PAZ, S. *Chem. Rev.* **2002**, *102*, 3667.
(10) Dahl, K.; Sando, G. M.; Fox, D. M.; Sutto, T. E.; Owrutsky, J. C. *J. Chem. Phys.* **2005**, 123.
(11) Hardacre, C.; Holbrey, J. D.; Nieuwenhuyzen, M.; Youngs, T. G. A. *Acc. Chem. Res.* **2007**, *40*, 1146.
(12) Urahata, S. M.; Ribeiro, M. C. C. *J. Chem. Phys.* **2005**, *122*, 024511.
(13) Shirota, H.; Funston, A. M.; Wishart, J. F.; Castner, E. W. *J. Chem. Phys.* **2005**, *122*, 184512.
(14) Earle, M. J.; Esperanca, J. M. S. S.; Gilea, M. A.; Lopes, J. N. C.; Rebelo, L. P. N.; Magee, J. W.; Seddon, K. R.; Widegren, J. A. *Nature (London)* **2006**, *439*, 831.
(15) Wishart, J. F.; Castner, E. W. *J. Phys. Chem. B* **2007**, *111*, 4639.
(16) Rogers, R. D.; Seddon, K. R. *Science* **2003**, *302*, 792.
(17) Brennecke, J. *Chem. Eng. News* **2001**, *79*, 86.
(18) Lee, S. Y.; Yong, H. H.; Lee, Y. J.; Kim, S. K.; Ahn, S. *J. Phys. Chem. B* **2005**, *109*, 13663.
(19) Garcia, B.; Lavallee, S.; Perron, G.; Michot, C.; Armand, M. *Electrochim. Acta* **2004**, *49*, 4583.
(20) Matsumoto, H.; Sakaebe, H.; Tatsumi, K. *J. Power Sources* **2005**, *146*, 45.
(21) Rivera, A.; Brodin, A.; Pugachev, A.; Rossler, E. A. *J. Chem. Phys.* **2007**, *126*, 114503.
(22) Wang, Y. T.; Voth, G. A. *J. Am. Chem. Soc.* **2005**, *127*, 12192.
(23) Wang, Y.; Jiang, W.; Yan, T.; Voth, G. A. *Acc. Chem. Res.* **2007**, *40*, 1193.
(24) Jiang, W.; Wang, Y. T.; Voth, G. A. *J. Phys. Chem. B* **2007**, *111*, 4812.
(25) Lopes, J. N. A. C.; Pádua, A. A. H. *J. Phys. Chem. B* **2006**, *110*, 3330.
(26) Hanke, C. G.; Lynden-Bell, R. M. *J. Phys. Chem. B* **2003**, *107*, 10873.
(27) Zhang, L. Q.; Xu, Z.; Wang, Y.; Li, H. R. *J. Phys. Chem. B* **2008**, *112*, 6411.
(28) Cammarata, L.; Kazarian, S. G.; Salter, P. A.; Welton, T. *Phys. Chem. Chem. Phys.* **2001**, *3*, 5192.
(29) Wang, Y.; Li, H. R.; Han, S. J. *J. Phys. Chem. B* **2006**, *110*, 24646.
(30) Lopez-Pastor, M.; Ayora-Canada, M. J.; Valcarcel, M.; Lendl, B. *J. Phys. Chem. B* **2006**, *110*, 10896.
(31) Huang, J. F.; Chen, P. Y.; Sun, I. W.; Wang, S. P. *Inorg. Chim. Acta* **2001**, *320*, 7.
(32) Jeon, Y.; Sung, J.; Seo, C.; Lim, H.; Cheong, H.; Kang, M.; Moon, B.; Ouchi, Y.; Kim, D. *J. Phys. Chem. B* **2008**, *112*, 4735.
(33) Fazio, B.; Triolo, A.; Di Marco, G. *J. Raman Spectrosc.* **2008**, *39*, 233.
(34) Jain, T. K.; Varshney, M.; Maitra, A. *J. Phys. Chem.* **1989**, *93*, 7409.
(35) Gao, Y.; Li, N.; Zheng, L. Q.; Zhao, X. Y.; Zhang, J.; Cao, Q.; Zhao, M. W.; Li, Z.; Zhang, G. Y. *Chem.—Eur. J.* **2007**, *13*, 2661.
(36) Kazarian, S. G.; Briscoe, B. J.; Welton, T. *Chem. Commun.* **2000**, 2047.
(37) Aki, S. N. V. K.; Brennecke, J. F.; Samanta, A. *Chem. Commun.* **2001**, 413.
(38) Tran, C. D.; Lacerda, S. H. D.; Oliveira, D. *Appl. Spectrosc.* **2003**, *57*, 152.
(39) Wang, J. J.; Pei, Y. C.; Zhao, Y.; Hu, Z. G. *Green Chem.* **2005**, *7*, 196.
(40) Widegren, J. A.; Laesecke, A.; Magee, J. W. *Chem. Commun.* **2005**, 1610.
(41) Widegren, J. A.; Saurer, E. M.; Marsh, K. N.; Magee, J. W. *J. Chem. Thermodyn.* **2005**, *37*, 569.
(42) Thomas, M.; Richardson, H. H. *Vib. Spectrosc.* **2000**, *24*, 137.
(43) Morita, S.; Shinzawa, H.; Noda, I.; Ozaki, Y. *J. Mol. Struct.* **2006**, *799*, 16.
(44) Richardson, H. H. *J. Mol. Struct.* **2006**, *799*, 56.
(45) Noda, I. *Appl. Spectrosc.* **1993**, *47*, 1329.
(46) Noda, I. *Appl. Spectrosc.* **2000**, *54*, 994.
(47) Noda, I.; Story, G. M.; Marcott, C. *Vib. Spectrosc.* **1999**, *19*, 461.

JP806805R